Journal of Catalysis 276 (2010) 66–75

Contents lists available at ScienceDirect

Journal of Catalysis

journal homepage: www.elsevier.com/locate/jcat

The formation of methane over iron catalysts applied in Fischer–Tropsch synthesis: A transient and steady state kinetic study

Barbara Graf, Hendrik Schulte, Martin Muhler *

Laboratory of Industrial Chemistry, Ruhr-University Bochum, Universitätsstr. 150, 44780 Bochum, Germany

ARTICLE INFO

Article history:
Received 12 May 2010
Revised 7 July 2010
Accepted 1 September 2010

Keywords:
CO pulse experiments
Methane formation
Bulk iron
Cementite
Potassium promoter
Fischer–Tropsch synthesis

ABSTRACT

The formation of methane over unpromoted and potassium-promoted bulk iron catalysts applied in Fischer–Tropsch synthesis (FTS) was studied by dosing carbon monoxide pulses in hydrogen. A bulk metallic iron catalyst was obtained by H_2 reduction, and cementite (Fe_3C)-containing but oxygen-free iron was prepared by exposure to methane. The pulse experiments yielded mainly CH_4 as well as small amounts of ethane and propane. The potassium-promoted samples reached higher degrees of CO conversion and lower CH_4 selectivities. The Fe_3C-containing catalysts were found to be more selective towards ethane and propane than reduced ones indicating that Fe_3C is more active in FTS than metallic iron. The pulse experiments resulted in different signal shapes of the CH_4 response curves reflecting the influence of the potassium promoter. The presence of potassium influenced the formation of CH_4 by blocking the fast formation channel and by establishing a new and slower reaction pathway, whereas the addition of potassium did not change the reaction pathway towards higher hydrocarbons. Therefore, the decreasing CH_4 formation rate contributes to the decreasing CH_4 selectivity with increasing potassium content found under high-pressure steady-state conditions. Pressure variation experiments at steady state revealed that the kinetic results obtained during the pulse experiments were reproduced at 1 bar. Gradual continuous changes in the product distribution were observed with increasing pressure allowing extrapolating the concepts obtained from experiments at atmospheric pressure to industrial high-pressure FTS conditions.

1. Introduction

Since many decades the Fischer–Tropsch synthesis (FTS) is an industrially established process for the production of mainly linear hydrocarbons with broad chain length distributions from synthesis gas [1,2]. Considering the continuously increasing crude oil price in recent years and severe environmental regulations concerning the sulphur content, it represents an alternative route for the production of petrochemical substitutes as well as high-quality fuels, because it can be based on several different synthesis gas feedstocks such as coal, natural gas, or biomass [3]. The high-temperature FTS is an iron-catalysed process with operation temperatures above 573 K aiming at the production of olefins and gasoline [4]. Frequently, an alkali promoter such as potassium is added to the iron catalyst for selectivity reasons [5]. Potassium increases the chain prolongation probability, lowers the CH_4 selectivity and increases the olefin selectivity [5–9].

The product distribution obtained by iron-catalysed FTS can generally be described by the Anderson–Schulz–Flory (ASF) distribution [10,11]. However, several experiments using iron-based catalysts reveal deviations from the ideal ASF distribution [12–14]. Therefore, the concept of a bimodal ASF distribution originating from the superposition of two ASF distributions with different chain growth probabilities was established. Madon and Taylor [12] attributed the different chain growth probabilities to at least two types of active sites. Gaube et al. [15] presented a study on alkali-promoted iron catalysts according to which only a certain fraction of the active sites is influenced by the alkali promoter. These sites are of a certain structure and possess a higher chain growth probability, whereas the unpromoted sites lead to the same growth probability as those on completely unpromoted iron catalysts.

A working iron catalyst under FTS conditions is a very complex system due to the coexisting phases and the wide product range. During the activation period of a metallic iron catalyst, a mixture of magnetite and iron carbides is formed [5]. Several iron-containing phases were found to be present in used iron catalysts after FTS [2,16–25]. The relative abundance of these phases is an individual parameter for each catalyst that depends on the pre-treatment and the reaction conditions [26]. Despite the ongoing discussion regarding the active sites, a correlation between the carbide content of the catalyst and its activity in FTS has been observed by several authors [20,27–36]. The presence of a potassium promoter is known to facilitate the activation of CO and the carbidization of iron oxide-containing catalyst precursors [7].

* Corresponding author. Fax: +49 234 32 14115.
E-mail address: muhler@techem.rub.de (M. Muhler).

0021-9517/$ - see front matter © 2010 Elsevier Inc. All rights reserved.
doi:10.1016/j.jcat.2010.09.001

Fe_3O_4 is accepted to catalyse the water gas shift reaction (WGSR) [37]. Many models describing the structure of an active iron FTS catalyst assume a core–shell system with a particle core consisting of Fe_3O_4 surrounded by an iron carbide shell [35,38–40].

The formation of CH_4 during FTS has to be suppressed for economical reasons. Several authors reported the presence of two active pools of surface intermediates during the methanation reaction on different catalysts [26,41–50]. Govender et al. [44] presented a SSITKA study on the formation of methane over an iron-based catalyst. They described two surface intermediates, which were both found to be active in the formation of methane and higher hydrocarbons. Matsumoto and Bennett [49] presented a transient study of the reaction intermediates present on a commercial iron catalyst at ambient pressure. They assumed CO_{ads} or C_{ads} to be the most likely intermediates for carbidization as well as methanation. Fournier et al. [26] reported on methanation experiments using an iron-based catalyst at ambient pressure. Methane was assumed to be formed via the surface carbide mechanism, and some smaller alkanes were also observed.

The present investigation into the methanation reaction via hydrogenation of CO during pulse experiments at ambient pressure provides information on the activity and selectivity of differently promoted iron catalysts as a function of the pre-treatment. Because of the complex composition of a working iron catalyst under FTS conditions, methane formation was either investigated over a bulk metallic iron catalyst, or a freshly reduced catalyst was first carbidized by means of methane resulting in the formation of Fe_3C, before the methanation reaction was started. Fe_3C is amongst the active phases reported for FTS [21]. The advantage of the generation of Fe_3C out of methane and reduced iron powder is the absence of an oxygen-containing iron phase. Therefore, it was possible to study the influence of catalyst carbidization on the methane selectivity without the superimposed reduction of iron oxides or the WGSR.

2. Experimental

2.1. The samples

The investigated bulk catalysts were unpromoted and potassium-promoted iron powder [51] with an average particle size of 1.35 μm. The iron powder was synthesized by decomposing iron carbonyl. The potassium-promoted samples were prepared by incipient wetness impregnation of Fe using K_2CO_3 as potassium source. The potassium contents were determined by atomic absorption spectroscopy (AAS). In the following, the unpromoted catalyst is labelled Fe, whereas the potassium-promoted samples are labelled according to their potassium contents of 0.20% and 0.96%, respectively (0.20% K/Fe, 0.96% K/Fe). The iron powder is an unsupported pore-free system with a BET surface area of approximately 0.25 $m^2\,g^{-1}$ after H_2 pre-treatment at 723 K.

2.2. Sample pre-treatment

Prior to all transient experiments, the samples were pre-treated by reduction for 13 h 40 min in a flow of 100 NmL min^{-1} H_2 at 723 K. The samples were purged for 20 min with He (100 NmL min^{-1}) at 723 K after reduction. One batch of samples was used in the pulse experiments directly after the reductive pre-treatment. The corresponding samples are denoted as Fe(red). In order to generate oxygen-free iron carbide species, a second batch of the samples was pre-treated in a flow of 80 NmL min^{-1} 50% CH_4/He at 723 K after reduction in hydrogen denoted as Fe(CH_4).

The samples used for the investigations at steady state were first purged in a flow of 500 NmL h^{-1} Ar at room temperature. Since the goal of high-temperature FTS consists in the production of olefins, all catalysts were pre-treated in H_2, since pre-treatment in CO or syngas is known to result in lower olefin selectivities [52]. Reduction was carried out for 5 h at 653 K in a flow of 500 NmL h^{-1} H_2 using a heating rate of 2 K min^{-1}. Afterwards, the samples were purged with Ar (500 NmL h^{-1}) and cooled to the reaction temperature of 613 K.

2.3. Pulse experiments

The flow set-up used for the pulse experiments consisted of a gas supply system including a dosing loop (V = 500 μL) for pulsing CO, a heated reactor and a calibrated quadrupole mass spectrometer (GAM 445, Balzers) for *on-line* gas analysis. The pulse experiments were carried out in a glass-lined stainless steel U-tube reactor with an inner diameter of 4 mm at 613 K using 1 g of sample of the sieve fraction of 250–355 μm. Fifty pulses of 10% CO/He were subsequently admitted into a flow of 30% H_2/He. The concentrations of the hydrogenation products (CH_4, H_2O, C_2H_6, C_3H_8) as well as the concentrations of CO and CO_2 were continuously analysed by means of the calibrated quadrupole mass spectrometer. The temperature was measured in the middle of the catalyst bed by a thermocouple, which was introduced into the reactor through a tee-piece.

2.4. Temperature-programmed oxidation (TPO)

In order to remove strongly bound carbon species from the catalyst, a TPO experiment was performed subsequent to the pulse experiments using the samples Fe(red), 0.20% K/Fe(red) and 0.96% K/Fe(red). The TPO experiments were performed in the temperature range from 303 K to 723 K using a heating rate of 12 K min^{-1} and a gas flow of 50 NmL min^{-1} 1% O_2/He. The product analysis of CO and CO_2 was performed continuously with the calibrated quadrupole mass spectrometer.

2.5. Steady-state experiments

The flow set-up used for the experiments at steady state consisted of three subunits: a gas supply system providing CO, H_2 and Ar, a heated reactor and a GC/MS for product analysis. Steady-state experiments at 613 K and a pressure of 25 bar (absolute) were carried out in a glass-lined stainless steel U-tube reactor with an inner diameter of 8 mm using the samples Fe, 0.20% K/Fe and 0.96% K/Fe. Additionally, a pressure variation in the pressure range from 25 bar to 1 bar was performed using the unpromoted iron catalyst. All experiments were carried out in a gas flow of 500 NmL h^{-1} 45% CO/45% H_2/10% Ar. Ar was used as internal standard for the GC/MS analysis. 500 mg of the Fe catalyst were diluted with SiC of the sieve fraction of 50–150 μm in the weight ratio 1:4, resulting in a bed height of 50 mm. In order to avoid product condensation, all lines and valves after the reactor were kept at a temperature of 463 K by means of a thermostated box. To protect the sensitive GC/MS system, long-chain hydrocarbons were deposited in a separator directly after leaving the reactor.

3. Results

The sample pre-treatment in H_2 yielded bulk metallic iron catalysts, whereas Fe_3C was the only iron carbide phase formed during the CH_4 pre-treatment. Fig. 1 shows the XRD patterns of the CH_4-pre-treated samples Fe(CH_4), 0.20% K/Fe(CH_4) and 0.96% K/Fe(CH_4). The comparison of the three patterns illustrates that

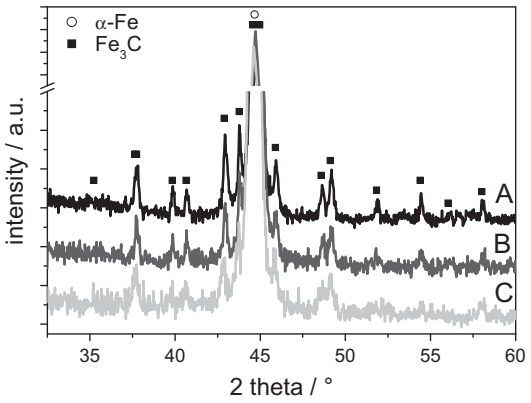

Fig. 1. XRD patterns of the CH_4-pre-treated samples: (A) Fe(CH_4), (B) 0.20% K/Fe(CH_4), and (C) 0.96% K/Fe(CH_4). The powder diffraction files of α-Fe (06-0696) and Fe_3C (72-1110) are included for comparison. The XRD patterns are shifted vertically.

all the samples consist of α-Fe and Fe_3C and that the intensity of the iron carbide reflexes decreased with increasing potassium content. It was not possible to carbidize the samples completely, that is, the XRD analysis always revealed residual α-Fe.

The normalized transient response curves of the components CH_4, H_2O, CO, CO_2 and C_2H_6 obtained during the hydrogenation of three CO pulses at 613 K are exemplarily shown for the reduced Fe sample in Fig. 2. The response curves of CH_4, CO, CO_2 and C_2H_6 consist of sharp peaks with high signal-to-noise ratios, whereas the H_2O traces are very broad with a low signal-to-noise ratio. The pulse experiments using the other samples resulted in qualitatively similar shapes of the response curves for the components H_2O, CO, CO_2 and C_2H_6 as shown in Fig. 2, whereas the shapes of the CH_4 traces differ strongly during the experiments. These differences are described and discussed in depth based on Fig. 3. The transient response curves of C_3H_8 are not included in Fig. 2, because only three of the investigated catalysts yielded C_3H_8. Therefore, it is not possible to find clear correlations between the potassium content of a catalyst and its transient C_3H_8 selectivity.

The transient response curves of CH_4 and C_2H_6 obtained during the hydrogenation of one CO pulse at 613 K over the different iron catalysts are shown in Fig. 3. Generally, the CH_4 response curves recorded for Fe(red) and Fe(CH_4) are most intensive. They consist of sharp signals in both cases (Fig. 3a), which show hardly any tailing and are almost as narrow as the CO and CO_2 responses (not

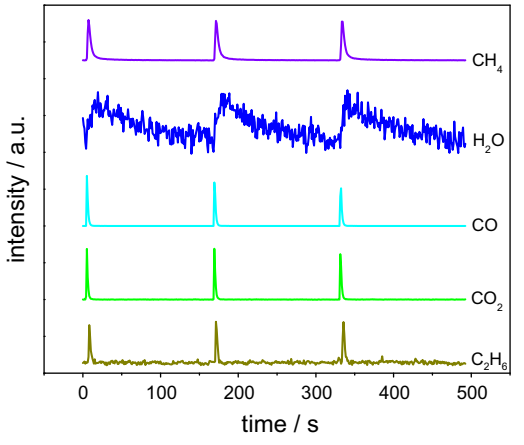

Fig. 2. Normalized transient response curves of the components CH_4, H_2O, CO, CO_2 and C_2H_6 obtained during the hydrogenation of three CO pulses at 613 K over Fe(red). All curves are shifted vertically for clarity. (For interpretation of the references to colour in this figure legend, the reader is referred to the web version of this article.)

shown). The transient response curves of CH_4 obtained for 0.20% K/Fe(red) and 0.20% K/Fe(CH_4) consist of a sharp first signal and a strongly tailing main signal (Fig. 3b). The strong tailing was also observed for 0.96% K/Fe(red), whereas the CH_4 responses of 0.96% K/Fe(CH_4) show tailing effects to a much lower extent (Fig. 3c). The sharp signal shape of the C_2H_6 response curves is qualitatively identical for all catalysts investigated (Fig. 3). Pre-carbidization of the catalysts led to higher C_2H_6 signal intensities.

The effluent amounts of CH_4, H_2O, CO, CO_2, C_2H_6 and C_3H_8 obtained during the hydrogenation of 50 pulses of CO at 613 K over the different iron catalysts are shown in Fig. 4. Particularly, the catalysts in the metallic iron state showed a temporal change of the effluent CO amount: during the admission of the first pulses, smaller amounts of CO were detected by the QMS, thus indicating higher degrees of CO conversion leading to the formation of stable carbon species on the surface or in the bulk. The presence of these very stable carbidic species on the potassium-promoted samples becomes evident from the TPO experiments, as described elsewhere. The pulse experiments using unpromoted Fe and 0.20% K/Fe yielded CH_4/H_2O ratios of 1:0.3 and 1:0.2, respectively, after reduction in H_2 and of 1:0.2 and 1:0.3, respectively, after the CH_4 treatment. The results obtained with 0.96% K/Fe differ from these observations. A CH_4/H_2O ratio of 1:2.5 was found after the H_2 pre-treatment, whereas it increased to 1:1.3 after the CH_4 treatment. This is a strong hint for the very strong carbidization tendency of these samples. The absolute amount of CO_2 formed decreased after the CH_4 pre-treatment of Fe and 0.20% K/Fe, whereas it increased after carbidization of 0.96% K/Fe. The pulse experiments also revealed the formation of C_2H_6 and C_3H_8 to a low extent. The samples 0.20% K/Fe(red), 0.96% K/Fe(red) and 0.96% K/Fe(CH_4) did not yield any C_3H_8.

All data required for solving the carbon and oxygen mass balances associated with the pulse experiments are shown in Fig. 5. Each diagram is divided into three parts. The first part shows the effluent amounts of the different components directly obtained from the pulse experiments after dosing 50 pulses of CO. The second part is only of relevance for the samples pre-treated in H_2 showing the amounts of CO and CO_2 formed during the TPO experiment. The summation of the effluent amounts of the first two parts is shown in part three based on the carbon balance: the first bar represents the calculated amount of CO dosed during 50 pulses, the second bar is equal to the amount of carbon-containing species formed during the pulse and TPO experiments, whereas the third bar is the amount of oxygen species formed during the pulse experiments.

The degrees of CO conversion as well as the individual selectivities of the different components obtained from the hydrogenation of 50 pulses of CO at 613 K over the different iron catalysts are summarized in Table 1 based on the carbon balance. For the samples 0.20% K/Fe(CH_4) and 0.96% K/Fe(CH_4), it was not possible to perform TPO experiments in order to solve the carbon mass balance, because the carbon species originating from the CH_4 pre-treatment or the CO pulses were indistinguishable. The highest degrees of CO conversion of up to 99% were obtained with the potassium-promoted catalysts. Over unpromoted Fe clearly much less CO was converted, especially after the pre-treatment in CH_4. The degrees of CO conversion obtained with the samples 0.96% K/Fe(red) and 0.96% K/Fe(CH_4) are in the same range as the CO conversion obtained with 0.20% K/Fe(red) and high compared to that of the unpromoted samples (Table 1, Fig. 4). Contrary to the other catalysts, the samples containing 0.96% potassium led to nearly identical CO conversion as well as CH_4 selectivity after reduction and CH_4 pre-treatment (Table 1). This observation suggests that these samples possess such a high CO dissociation tendency that most of the converted CO leads to the carbidization of the catalyst. Despite the high degrees of CO conversion, no temperature

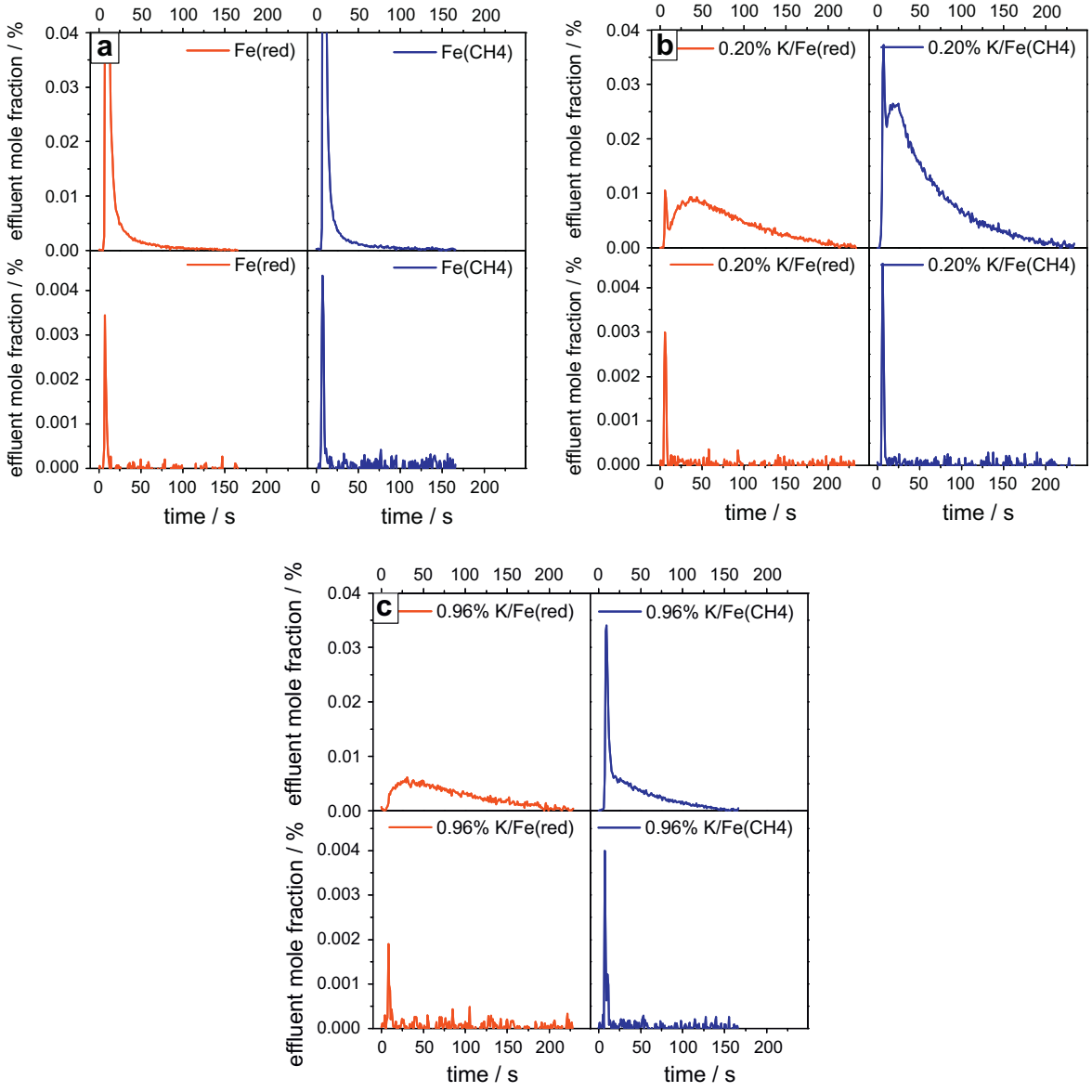

Fig. 3. Transient response curves of CH_4 (top) and C_2H_6 (bottom) obtained during the hydrogenation of one CO pulse at 613 K over (a) Fe(red) and Fe(CH_4), (b) 0.20% K/Fe(red) and 0.20% K/Fe(CH_4) and (c) 0.96% K/Fe(red) and 0.96% K/Fe(CH_4). (For interpretation of the references to colour in this figure legend, the reader is referred to the web version of this article.)

gradient was present during the pulse experiments as indicated by the thermocouple placed in the catalyst bed.

The CH_4 selectivities show the opposite trend: they are high in case of Fe(red) and Fe(CH_4), whereas they decrease for the potassium-promoted samples. The highest selectivities of C_2H_6 and C_3H_8 were obtained with the unpromoted catalyst, and a selectivity decrease was observed with increasing potassium content. Generally, the CH_4-pre-treated catalysts showed higher C_2H_6 and C_3H_8 selectivities. It has to be pointed out that these results were obtained at non-steady-state conditions, because the partial pressures of both the reactants and products changed rapidly during each pulse.

The results of the steady-state experiments at 25 bar are shown in Figs. 6 and 7. Full conversion of CO was reached with all samples. The presence of potassium suppressed CH_4 formation, increased the chain prolongation probability and decreased the selectivity to the desired C_2 to C_4 hydrocarbons (Fig. 6). On the other hand, the olefinicity is strongly increased in case of the potassium-promoted samples. An increase in the potassium content from 0.20% to 0.96% affects the olefin selectivity only slightly (Fig. 7).

As an attempt to bridge the pressure gap between the pulse experiments at atmospheric pressure and the steady-state investigations at 25 bar, a pressure variation was carried out. The hydrocarbon selectivities obtained with the unpromoted iron catalyst at steady state are shown in Fig. 8. The results reveal two remarkable trends. First, the CH_4 selectivity strongly decreases from 43.8% at 1 bar to 14.8% at 25 bar. Second, the ratio of the C_2 and C_3 selectivities depends on the pressure: in the pressure range from 1 bar to 10 bar, the C_2 selectivity is higher than the C_3 selectivity, whereas this ratio is inverted at 25 bar.

4. Discussion

4.1. Catalyst carbidization by CH_4 and CO

The formation of Fe_3C during the CH_4 pre-treatment of the reduced iron catalysts occurred according to $3Fe + CH_4 \leftrightarrows Fe_3C + 2H_2$. It is known that Fe_2C and $Fe_{2.2}C$ are formed simultaneously

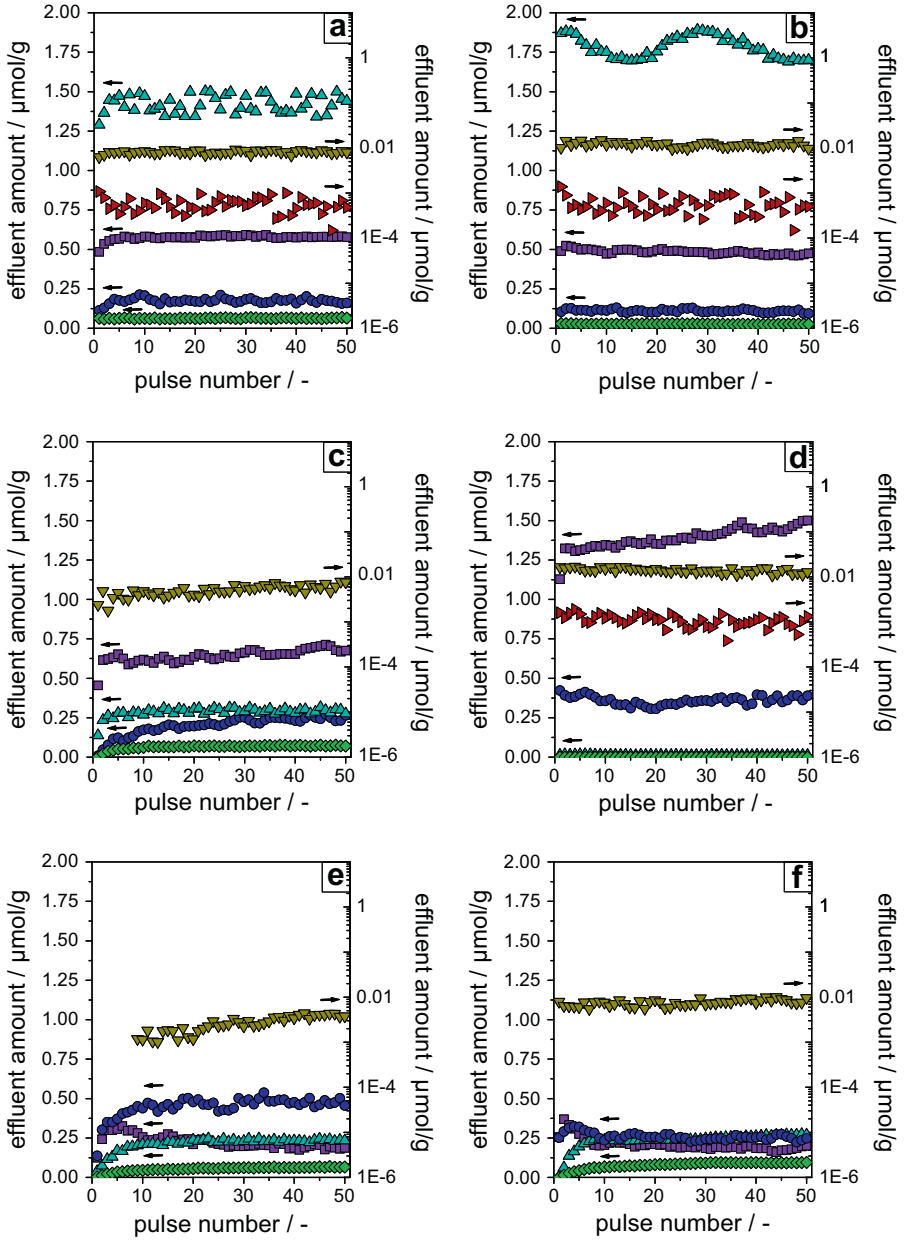

Fig. 4. Effluent amounts of the components CH_4 (■), H_2O (●), CO (▲), CO_2 (♦), C_2H_6 (▼) and C_3H_8 (▶) obtained during the hydrogenation of 50 pulses of CO at 613 K over (a) Fe(red), (b) Fe(CH_4), (c) 0.20% K/Fe(red), (d) 0.20% K/Fe(CH_4), (e) 0.96% K/Fe(red), and (f) 0.96% K/Fe(CH_4). (For interpretation of the references to colour in this figure legend, the reader is referred to the web version of this article.)

in the low temperature range (388 K), whereas at 423 K to 458 K only Fe_2C is formed. These iron carbide phases are converted to Fe_5C_2 at temperatures of 493 K to 673 K. The stable phase above 723 K is Fe_3C [28]. Our experimental approach to generate an oxygen-free iron carbide sample is based on the decomposition of CH_4. Due to its stability, it is not possible to produce iron carbide phases in the low temperature range. Indeed, Fe_3C was formed under the chosen experimental conditions at 723 K. Since no baseline drift of the CH_4 signal was observed during the CO pulse experiments in H_2, it can be concluded that the generated iron carbide phase is stable under our experimental conditions. However, it was not possible to carbidize the catalysts completely. According to Li et al. [34,39], it is sufficient to convert the outer surface layers into iron carbides to achieve FTS activity. The catalytic behaviour of these dynamic surface layers is not influenced by the chemical composition of the iron cores of the catalyst particles. The carbidized fraction after the CH_4 treatment was even lower in case of the potassium-promoted catalysts in agreement with the literature [53]. The low degree of carbidization is reasonable, because the dissociative adsorption of CH_4 on iron is the rate-limiting step in iron carbide formation [54]. Another difficulty in carbidizing the iron catalysts completely is their particle size, as smaller iron particles are known to carbidize more rapidly and completely than larger particles [55].

The sample 0.96% K/Fe(CH_4) was the least carbidized sample when performing the CH_4 pre-treatment (Fig. 1). Therefore, residual sites necessary for the formation of interstitial iron carbides were still available. Due to its high potassium content, the sample 0.96% K/Fe possesses a high CO dissociation tendency. Because of the potassium promoter effect [56], iron carbide formation is more favoured in case of using CO as carbon source compared to using CH_4. Therefore, residual sites were occupied by carbon atoms

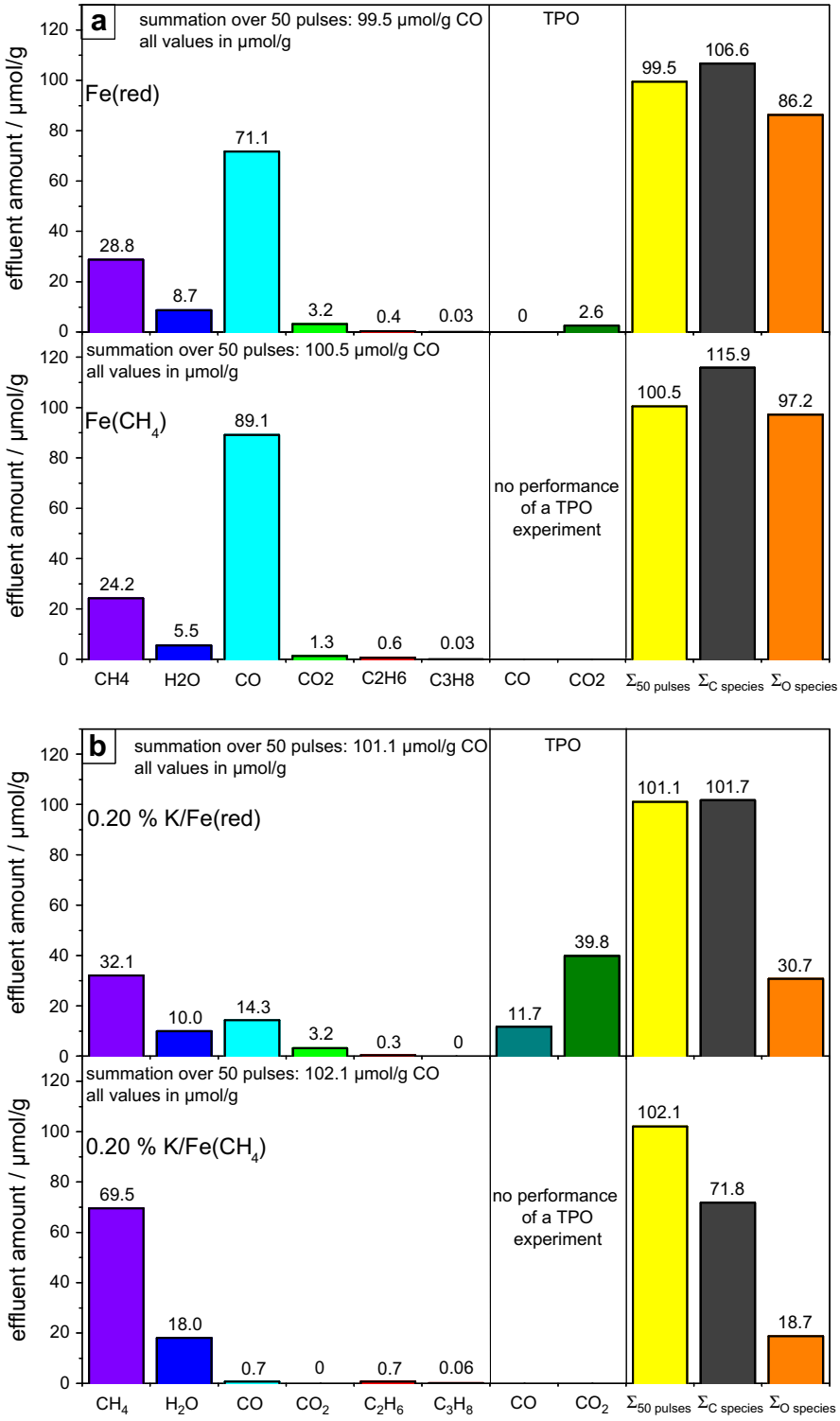

Fig. 5. Effluent amounts of gaseous compounds detected during the hydrogenation of 50 pulses of CO at 613 K and the TPO experiments, respectively, using (a) Fe(red) and Fe(CH_4), (b) 0.20% K/Fe(red) and 0.20% K/Fe(CH_4) and (c) 0.96% K/Fe(red) and 0.96% K/Fe(CH_4). (For interpretation of the references to colour in this figure legend, the reader is referred to the web version of this article.)

during the pulse experiments even after CH_4 pre-treatment of the catalyst. The low degrees of CO conversion obtained with the samples Fe(red) and Fe(CH_4) (Table 1) indicate a low ability of these samples to dissociate CO and form iron carbides, which is ascribed to a much weaker Fe–C bond than in case of the potassium-promoted samples [56]. Due to the weak Fe–C interaction, high CH_4 selectivities were observed, because nearly all carbon reacting over the catalysts was converted to gaseous compounds, especially CH_4.

The degrees of CO conversion obtained with the potassium-promoted samples (Table 1) are high compared to the CO conversion of the unpromoted samples. The higher degrees of CO conversion reflect the higher carbidization tendency of the potassium-

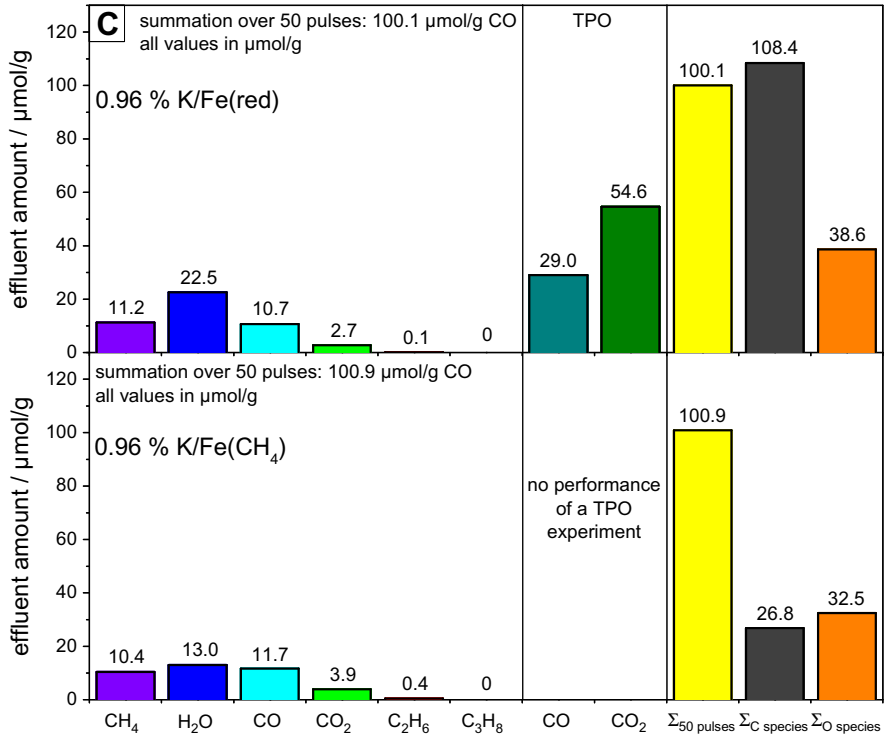

Fig. 5 (*continued*)

Table 1
Degrees of CO conversion and individual selectivities of the different components obtained from the pulse experiments.

	X_{CO} (%)	S_{CH4} (%)	S_{C2H6} (%)	S_{C3H8} (%)	S_{CO2} (%)	$S_{CO\ (TPO)}$ (%)	$S_{CO2\ (TPO)}$ (%)	$\sum_{select.}$ (%)
Fe(red)	33.30	81.13	2.25	0.25	9.01	–	7.32	99.96
Fe(CH_4)	23.12	90.30	4.48	0.34	4.85	–	–	99.97
0.20% K/Fe(red)	85.86	36.98	0.69	–	3.69	13.48	45.85	100.69
0.20% K/Fe(CH_4)	99.31	68.54	1.38	0.18	–	–	–	70.10
0.96% K/Fe(red)	90.13	11.46	0.20	–	2.76	29.68	55.89	99.99
0.96% K/Fe(CH_4)	88.40	11.66	0.90	–	4.37	–	–	16.93

– = Component was not formed.

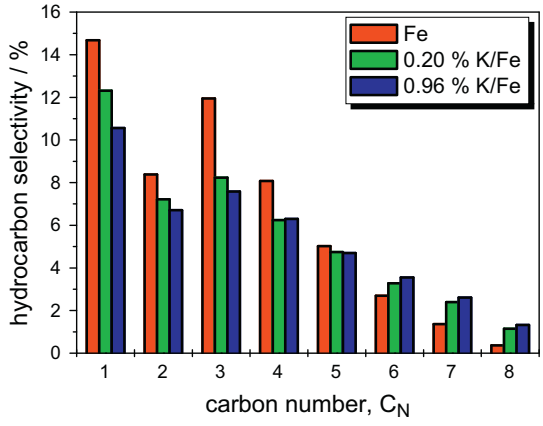

Fig. 6. Hydrocarbon selectivities obtained with the samples Fe, 0.20% K/Fe and 0.96% K/Fe in the steady-state experiments at 25 bar and 613 K (H_2:CO = 1:1).

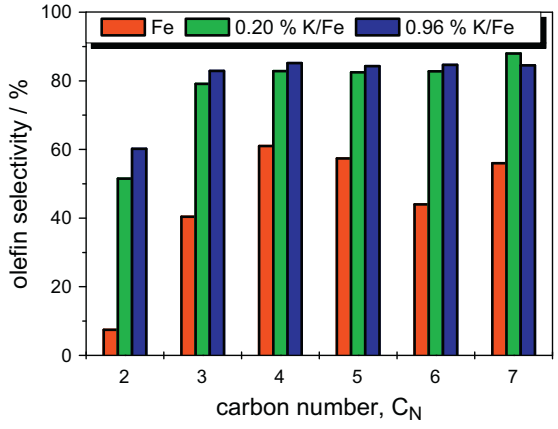

Fig. 7. Olefin selectivities obtained with the samples Fe, 0.20% K/Fe and 0.96% K/Fe in the steady-state experiments at 25 bar and 613 K (H_2:CO = 1:1).

promoted samples due to the facilitated CO dissociation. The carbidization tendency of 0.96% K/Fe is even stronger than the oxophilicity of reduced iron. Therefore, the samples with a potassium content of 0.96% are not very suitable for the investigation of the CH_4 formation, because the deactivation tendency is too strong.

In contrast to results reported in literature [26], the formation of larger amounts of strongly bound carbon species only occurred on the potassium-promoted samples. Fournier et al. [26] found 10 wt.% of free carbon species present on a spent iron-based methanation catalyst. However, the TPO experiment subsequent

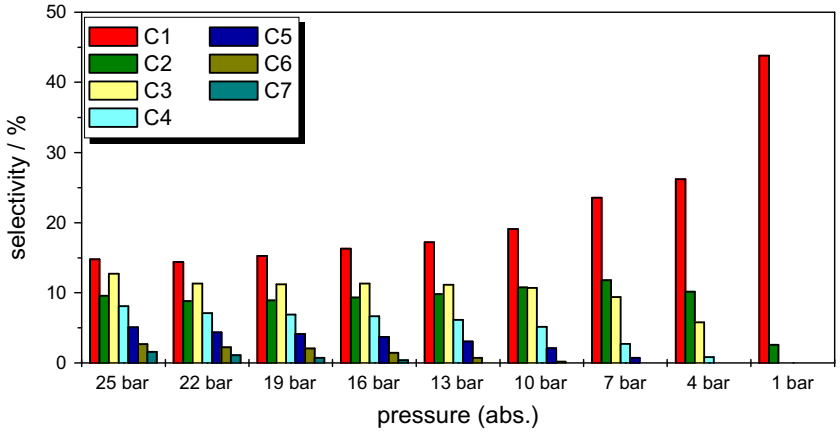

Fig. 8. Hydrocarbon selectivities obtained with the unpromoted iron catalyst in the steady-state experiments during pressure variation from 25 bar to 1 bar (613 K, H_2:CO = 1:1).

to the pulse experiment using the Fe(red) sample detected only 2.6 μmol g^{-1} of strongly bound carbon species. This is equivalent to approximately 2.4% of the dosed CO amount, again due to our experimental conditions.

Because of the excess of H_2 present during the pulse experiments, a competition between the direct hydrogenation of surface carbon species and diffusion into the bulk has to be considered, which is different from typical FTS conditions, where the rate of carbon diffusion is reported to be higher than the rate of the hydrogenation reaction [55]. The TPO experiment performed subsequent to the pulse experiment using 0.20% K/Fe(red) revealed that approximately 50% of the dosed CO molecules were converted to stable carbidic species only removable by oxygen. The results of the pulse experiments presented in Fig. 4b indicate that these carbon species do not lower the catalytic activity. The effluent amounts of the components CH_4, H_2O, CO, CO_2 and C_2H_6 obtained during the pulse experiments do not indicate any deactivation behaviour of the catalyst, either. This should be expected in case of graphitic carbon species present on the surface. Comparative TPO experiments (not shown) using a separate batch of freshly prepared 0.20% K/Fe(CH_4) containing Fe_3C revealed that these carbon species are in fact carbidic. Considering the results reported by Krebs et al. [57], the graphite formation tendency during the pulse experiments should indeed be really low, since it depends on the CO/H_2 ratio. A decreasing CO/H_2 ratio generally leads to an increasing onset temperature of extensive graphite formation. For a CO/H_2 ratio of 1:100 graphite formation started at 655 K, whereas lower temperatures only lead to iron carbide formation.

Although Bukur et al. [58] reported that potassium contents of up to 1% were beneficial for FT activity, our results imply a strong carbidization tendency of the catalyst containing 0.96% potassium and that the balance between activity increase and deactivation of the catalyst is already exceeded, presumably due to the very low iron surface area of our samples. Only 24.8 μmol g^{-1} and 26.8 μmol g^{-1} carbon-containing species were detected during the pulse experiments using 0.96% K/Fe(red) and 0.96% K/Fe(CH_4), respectively (Fig. 5c), which corresponds to only one-fourth of the dosed CO amount. During the TPO experiment subsequent to the pulse experiment using 0.96% K/Fe(red), 83.6 μmol g^{-1} carbon-containing species were released. These species were identified to be a mixture of coke and Fe_3C by a TPO experiment (not shown) using freshly carbidized 0.96% K/Fe(CH_4).

4.2. State of the catalysts during the pulse experiments

The broad H_2O response curves obtained during the pulse experiments (Fig. 2) indicate slow H_2O desorption from the unpromoted catalysts compared to CH_4 and CO_2 desorption. This observation was also reported in the literature for cobalt-based catalysts. Khodakov et al. [50] presented transient studies of the elementary steps in the cobalt-catalysed FTS. They found that H_2O desorption from cobalt was much slower than the hydrogenation of surface carbon species. The broad shape of the H_2O response curves is independent of the pre-treatment conditions and the potassium content. All H_2O signals recorded during our pulse experiments looked qualitatively similar (not shown) always reaching the baseline again. Therefore, the catalyst surface is in an oxygen-free state at the beginning of each CO pulse. Because the oxygen mass balance was not closed for any of the pulse experiments (Fig. 5), it is assumed that a shell of iron oxide is formed in the near-surface region of the iron catalysts.

A marginal amount of CO_2 was also formed during the pulse experiments (Fig. 5). Possible reaction pathways leading to CO_2 are the WGSR and the Fe_3C formation according to

$$2CO + 3Fe \rightarrow Fe_3C + CO_2 \quad (1)$$

or

$$3CO + 6Fe + H_2 \rightarrow 2Fe_3C + CO_2 + H_2O \quad (2)$$

Due to the closed carbon mass balance for the sample Fe(CH_4) (Fig. 5a), Fe_3C formation and associated CO_2 formation can be excluded. The carbon mass balance for Fe(CH_4) was closed only by the data obtained from the pulse experiment, whereas some oxygen was missing. In the case of Fe_3C formation from CO, carbon would remain on the catalyst and, as a consequence, it would be missing in the carbon mass balance. Therefore, the CO_2 formation observed during the pulse experiments is assumed to be due to a slight WGS activity of the catalysts. According to literature, Fe_3O_4, and not FeC_x, is the active phase for the WGSR [37]. Therefore, Fe_3O_4 formation must have occurred to some extent, since both samples were oxygen-free at the beginning of each pulse experiment (Fig. 1). In our studies, the oxygen necessary for Fe_3O_4 formation results from dissociative CO adsorption. Since the partial oxidation of reduced iron is generally more favoured than oxidation of the iron carbides [59], the reduced sample is slightly more active in the WGSR, which is consistent with the concept of a shell of iron oxide in the near-surface region. The concept is also valid for the 0.20% K/Fe samples.

4.3. Influence of the potassium promoter on the CH_4 and C_2H_6 formation rates

The transient response curves of CH_4 obtained during the hydrogenation of a CO pulse at 613 K (Fig. 3) show two general

shapes, which are considered as two border cases. On the one hand, very sharp and narrow response signals were obtained using Fe(red) and Fe(CH_4). On the other hand, the pulse experiment over 0.96% K/Fe(red) led to very broad signals with relatively low signal-to-noise ratios. The CH_4 responses obtained with the unpromoted samples indicate very fast hydrogenation and weakly bound adsorbates. In fact, the broad shape of the CH_4 signals recorded using 0.96% K/Fe(red) is a sign for a decelerated CH_4 formation process. Since it is known that CH_4 readsorbs neither on metallic iron [60,61] nor on iron carbides [44,62], the signal broadening is not due to readsorption effects. Instead, the different signal shapes are attributed to the influence of the potassium promoter, which leads to a slower CH_4 formation rate. The determination of the full width at half maximum for the transient CH_4 response curves of Fe(red) and 0.96% K/Fe(red) yielded values of 4 s and 120 s corresponding to a difference by a factor of 30. The sharp signals obtained using the unpromoted catalysts are assigned to fast CH_4 formation on non-alkalized sites, whereas the very broad CH_4 response curve observed for 0.96% K/Fe(red) indicates a slower CH_4 formation rate on alkali-promoted sites. The pulse experiments using 0.20% K/Fe(red) and 0.20% K/Fe(CH_4) led to CH_4 response curves, which point to the coexistence of alkali-promoted as well as unpromoted active sites in agreement with the results obtained by Gaube et al. [15]. The sharp first signal is qualitatively identical to the one obtained on the unpromoted samples and therefore assigned to CH_4 formation on non-alkalized sites. The broad part of the CH_4 response curve resembles the one obtained using 0.96% K/Fe(red) resulting from the CH_4 formation on alkalized sites. Therefore, the CH_4 signals observed during the transient pulse experiments on 0.20% K/Fe(red) and 0.20% K/Fe(CH_4) are superimposed signals. The potassium promoter influences the CH_4 formation by establishing a new and slower reaction pathway without changing the reaction pathway towards ethane. This becomes evident from the transient C_2H_6 response curves shown in Fig. 3. The decreasing CH_4 formation rate contributes to the decreasing CH_4 selectivity obtained with potassium-promoted iron catalysts. The fast CH_4 formation channel is completely blocked using 0.96% K/Fe(red) and at least partially blocked in case of the other potassium-promoted catalysts. The two different CH_4 formation pathways were also observed after pre-carbidization of the potassium-containing catalysts.

4.4. Selectivity towards higher hydrocarbons

The highest ethane and propane selectivities were obtained with the unpromoted catalysts. This is contrary to the FTS product distributions obtained under high-pressure conditions, where potassium increases the chain prolongation probability and shifts the product spread towards higher hydrocarbons (Fig. 6). These deviations from the expected ethane and propane product distributions originate from the reaction pressure and the very low CO/H_2 ratio applied in our studies. Due to the missing potassium promoter effect in the samples Fe(red) and Fe(CH_4), the carbon-containing surface species are comparatively weakly bound, and the hydrocarbons possess an increased formation and desorption tendency.

The pulse experiments also revealed that Fe_3C is more selective in the formation of higher hydrocarbons than metallic iron, as the three investigated catalysts yielded higher selectivities of C_2H_6 after CH_4 treatment (Table 1). Additionally, an increased C_3H_8 selectivity was observed for the samples Fe(CH_4) and 0.20% K/Fe(CH_4). Due to the increasing carbidization tendency of iron catalysts with increasing potassium content, the pulse experiments using 0.96% K/Fe(red) as well as 0.96% K/Fe(CH_4) yielded the lowest selectivities of C_2H_6 and no formation of C_3H_8 (Table 1). The adsorbed carbon species are obviously bound too strongly resulting in very low reaction and desorption probabilities.

4.5. Experiments at steady state

The results of the pulse experiments were confirmed during measurements at steady state. The lower CH_4 formation tendency of the potassium-promoted iron catalysts observed during FTS at 25 bar (Fig. 6) is on the one hand due to an increasing growth probability of the hydrocarbon fragments on these samples. The growth probability can be calculated according to the model of Anderson et al. [11]. A value of 0.47 was obtained for the unpromoted iron catalysts, whereas the growth probabilities of the potassium-promoted samples amount to 0.59 (0.20% K/Fe) and 0.61 (0.96% K/Fe). On the other hand, the slower CH_4 formation pathway on the potassium-promoted iron catalysts is assumed to be accessible also at 25 bar. The fast CH_4 formation channel is at least partially blocked. The strongly increasing olefin selectivity of the potassium-promoted catalysts can be rationalized by means of a model reported by Gaube and Klein [63]. Due to the potassium promoter effect, the adsorption strength of CO increases causing an enhanced displacement of adsorbed alkenes compared to an unpromoted iron catalyst.

The pressure variation experiments at steady state are an attempt to bridge the pressure gap between the pulse experiments at 1 bar and the steady-state investigations at 25 bar. The product distribution obtained during the pulse experiments was reproduced during the steady-state experiment at 1 bar, indicating that C-C coupling is also hardly occurring under flow conditions. However, gradual continuous changes were observed with increasing pressure, for instance the crossing of the C_2 and C_3 selectivities, which can probably be rationalized by two aspects: first, an increasing chain growth probability with increasing pressure and second, an increasing incorporation tendency of C_2 olefins into growing chains with increasing pressure. Although a strong pressure dependence of the product distribution exists, an extrapolation of the concepts obtained from the pulse experiments at atmospheric pressure to high-pressure FTS conditions is considered feasible. Further studies concerning the influence of the potassium promoter on the kinetics and thermodynamics of bulk iron catalysts using temperature-programmed desorption and surface hydrogenation and adsorption calorimetry are in progress.

5. Conclusions

The formation of methane on either unpromoted or potassium-promoted iron catalysts was studied by hydrogenating CO applying CO pulses in flowing H_2 after different catalyst pre-treatments. The CH_4 pre-treatment was chosen in order to simplify the multi-component system of a working FTS iron catalyst resulting in the formation of Fe_3C. Therefore, it was possible to study the hydrogenation of CO without the superimposed effects of iron oxides such as reduction or the water gas shift reaction. The main product formed during the pulse experiments was CH_4, and small amounts of ethane and propane were observed in addition. Since our experimental conditions led to a limited product distribution, it was possible to close the carbon mass balances. In the case of the potassium-promoted catalysts, this was only possible after the removal of strongly bound carbidic carbon species by means of subsequent TPO experiments. The degrees of CO conversion obtained with the potassium-promoted samples were high pointing to facilitated dissociative CO adsorption.

The different signal shapes of the transient CH_4 response curves indicate that only a certain fraction of the active sites is influenced by the potassium promoter at medium potassium contents. The

fast CH_4 formation channel is at least partially blocked, and the potassium-promoted sites open a new and slower reaction pathway towards methane without influencing the reaction pathway towards higher hydrocarbons. Therefore, it can be concluded that the decreasing CH_4 formation rate contributes to the decreasing CH_4 selectivity with increasing potassium content also found under high-pressure FTS conditions. The pre-carbidization of the catalysts was observed to have an effect only on the selectivity towards higher hydrocarbons, whereas an influence on the different CH_4 formation pathways was not found.

Also during the experiments at steady state at 25 bar, potassium was found to suppress CH_4 formation. Additionally, the presence of potassium led to a strongly increased olefin selectivity pointing to an enhanced alkene desorption rate. The pressure variation experiments at steady state revealed a strongly decreasing CH_4 selectivity in the pressure range from 1 bar to 25 bar and a crossing of the C_2 and C_3 selectivities. Due to these gradual continuous changes, an extrapolation of the concepts based on the pulse experiments performed at atmospheric pressure to industrial Fischer–Tropsch conditions is considered feasible.

Acknowledgment

Financial support by BASF SE and by the Fonds der Chemischen Industrie (FCI) is gratefully acknowledged. The authors thank Dr. J. Steiner and Dr. E. Schwab (BASF SE) for fruitful discussions.

References

[1] H. Schulz, Appl. Catal. A 186 (1999) 3.
[2] T. Herranz, S. Rojas, F.J. Pérez-Alonso, M. Ojeda, P. Terreros, J.L.G. Fierro, J. Catal. 243 (2006) 199.
[3] C.H. Bartholomew, R.J. Farrauto, Fundamentals of Industrial Catalytic Processes, Wiley-Interscience, 2006. pp. 398.
[4] M.E. Dry, Appl. Catal. A 276 (2004) 1.
[5] M.E. Dry, in: J.R. Anderson, M. Boudart (Eds.), Catalysis: Science and Technology, Springer, Berlin, 1981, pp. 159.
[6] S. Li, S. Krishnamoorthy, A. Li, G.D. Meitzner, E. Iglesia, J. Catal. 206 (2002) 202.
[7] S. Li, A. Li, S. Krishnamoorthy, E. Iglesia, Catal. Lett. 77 (2001) 197.
[8] S.L. Soled, E. Iglesia, S. Miseo, B.A. DeRites, R.A. Fiato, Top. Catal. 2 (1995) 193.
[9] M. Luo, B.H. Davis, Appl. Catal. A 246 (2003) 171.
[10] G. Henrici-Olivé, S. Olivé, Angew. Chem. 88 (1976) 144.
[11] R.B. Anderson, R.A. Friedel, H.H. Storch, J. Chem. Phys. 19 (1951) 313.
[12] R.J. Madon, W.F. Taylor, J. Catal. 69 (1981) 32.
[13] G.A. Huff jr., C.N. Satterfield, J. Catal. 85 (1984) 370.
[14] L. König, J. Gaube, Chem.-Ing.-Tech. 55 (1983) 14.
[15] J. Gaube, K. Herzog, L. König, B. Schliebs, Chem.-Ing.-Tech. 58 (1986) 682.
[16] D.J. Dwyer, G.A. Somorjai, J. Catal. 52 (1978) 291.
[17] C.S. Kuivila, P.C. Stair, J.B. Butt, J. Catal. 118 (1989) 299.
[18] J.P. Reymond, P. Mériaudeau, S.J. Teichner, J. Catal. 75 (1982) 39.
[19] E. de Smit, A.M. Beale, S. Nikitenko, B.M. Weckhuysen, J. Catal. 262 (2009) 244.
[20] K.R.P.M. Rao, F.E. Huggins, V. Mahajan, G.P. Huffman, V.U.S. Rao, B.L. Bhatt, D.B. Bukur, B.H. Davis, R.J. O'Brien, Top. Catal. 2 (1995) 71.
[21] J.F. Shultz, W.K. Hall, T.A. Dubs, R.B. Anderson, J. Am. Chem. Soc. 78 (1956) 282.
[22] G. LeCaër, J.M. Dubois, M. Pijolat, V. Perrichon, P. Bussière, J. Phys. Chem. 86 (1982) 4799.
[23] L.D. Mansker, Y. Jin, D.B. Bukur, A.K. Datye, Appl. Catal. A 186 (1999) 277.
[24] J.W. Niemantsverdriet, A.M. van der Kraan, W.L. van Dijk, J.S. van der Baan, J. Phys. Chem. 84 (1980) 3363.
[25] R.A. Dictor, A.T. Bell, J. Catal. 97 (1986) 121.
[26] J. Fournier, L. Carreiro, Y.-T. Qian, S. Soled, R. Kershaw, K. Dwight, A. Wold, J. Solid State Chem. 58 (1985) 211.
[27] A. Sarkar, D. Seth, A.K. Dozier, J.K. Neathery, H.H. Hamdeh, B.H. Davis, Catal. Lett. 117 (2007) 1.
[28] J.A. Amelse, J.B. Butt, L.H. Schwartz, J. Phys. Chem. 82 (1978) 558.
[29] R.J. O'Brien, L. Xu, R.L. Spicer, B.H. Davis, Energy Fuels 10 (1996) 921.
[30] T. Riedel, H. Schulz, G. Schaub, K.-W. Jun, J.-S. Hwang, K.-W. Lee, Top. Catal. 26 (2003) 41.
[31] J.W. Niemantsverdriet, A.M. van der Kraan, J. Catal. 72 (1981) 385.
[32] M.D. Shroff, D.S. Kalakkad, K.E. Coulter, S.D. Köhler, M.S. Harrington, N.B. Jackson, A.G. Sault, A.K. Datye, J. Catal. 156 (1995) 185.
[33] S. Li, R.J. O'Brien, G.D. Meitzner, H. Hamdeh, B.H. Davis, E. Iglesia, Appl. Catal. A 219 (2001) 215.
[34] S. Li, G.D. Meitzner, E. Iglesia, J. Phys. Chem. B 105 (2001) 5743.
[35] B.H. Davis, Catal. Today 141 (2009) 25.
[36] Y. Zhang, N. Sirimanothan, R.J. O'Brien, H.H. Hamdeh, B.H. Davis, Stud. Surf. Sci. Catal. 139 (2001) 125.
[37] G.P. van der Laan, A.A.C.M. Beenackers, Catal. Rev. – Sci. Eng. 41 (1999) 255.
[38] S. Li, G.D. Meitzner, E. Iglesia, Stud. Surf. Sci. Catal. 136 (2001) 387.
[39] S. Li, W. Ding, G.D. Meitzner, E. Iglesia, J. Phys. Chem. B 106 (2002) 85.
[40] B.H. Davis, Catal. Today 84 (2003) 83.
[41] J. Happel, I. Suzuki, P. Kokayeff, V. Fthenakis, J. Catal. 65 (1980) 59.
[42] J. Happel, H.Y. Cheh, M. Otarod, S. Ozawa, A.J. Severdia, T. Yoshida, V. Fthenakis, J. Catal. 75 (1982) 314.
[43] M. Otarod, S. Ozawa, F. Yin, M. Chew, H.Y. Cheh, J. Happel, J. Catal. 84 (1983) 156.
[44] N.S. Govender, F.G. Botes, M.H.J.M. de Croon, J.C. Schouten, J. Catal. 260 (2008) 254.
[45] M. Otarod, J. Happel, E. Walter, Appl. Catal. A 160 (1997) 3.
[46] Y. Soong, K. Krishna, P. Biloen, J. Catal. 97 (1986) 330.
[47] I.-G. Bajusz, J.G. Goodwin Jr., J. Catal. 169 (1997) 157.
[48] M.W. Balakos, S.S.C. Chuang, G. Srinivas, M.A. Brundage, J. Catal. 157 (1995) 51.
[49] H. Matsumoto, C.O. Bennett, J. Catal. 53 (1978) 331.
[50] A.Y. Khodakov, B. Peregryn, A.S. Lermontov, J.-S. Girardon, S. Pietrzyk, Catal. Today 106 (2005) 132.
[51] B.W. Hoffer, S. Bunzel, D. Neumann, K. Bay, E. Schwab, U. Grässle, J. Steiner, Patent PCT/EP2008/059207, 2008.
[52] M. Luo, B.H. Davis, Fuel Process. Technol. 83 (2003) 49.
[53] U. Narkiewicz, I. Kucharewicz, A. Pattek-Janczyk, W. Arabczyk, Rev. Adv. Mater. Sci. 8 (2004) 59.
[54] W. Arabczyk, W. Konicki, U. Narkiewicz, I. Jasinska, K. Kalucki, Appl. Catal. A 266 (2004) 135.
[55] E. de Smit, B.M. Weckhuysen, Chem. Soc. Rev. 37 (2008) 2758.
[56] M.E. Dry, T. Shingles, L.J. Boshoff, G.J. Oosthuizen, J. Catal. 15 (1969) 190.
[57] H.J. Krebs, H.P. Bonzel, G. Gafner, Surf. Sci. 88 (1979) 269.
[58] D.B. Bukur, D. Mukesh, S.A. Patel, Ind. Eng. Chem. Res. 29 (1990) 194.
[59] X.Q. Zhao, Y. Liang, Z.Q. Hu, B.X. Liu, J. Appl. Phys. 80 (1996) 5857.
[60] G. Wedler, M. Mengel, Surf. Sci. 131 (1983) L423.
[61] D.C. Sorescu, Phys. Rev. B 73 (2006) 155420–155421.
[62] D.-B. Cao, Y.-W. Li, J. Wang, H. Jiao, J. Phys. Chem. C 112 (2008) 14883.
[63] J. Gaube, H.-F. Klein, Appl. Catal. A 350 (2008) 126.